Proteomic and bioinformatic analyses of spinal cord injury-induced skeletal muscle atrophy in rats

ZHI-JIAN WEI[*], XIAN-HU ZHOU[*], BAO-YOU FAN, WEI LIN, YI-MING REN and SHI-QING FENG

Department of Orthopaedics, Tianjin Medical University General Hospital, Tianjin 300052, P.R. China

Abstract. Spinal cord injury (SCI) may result in skeletal muscle atrophy. Identifying diagnostic biomarkers and effective targets for treatment is an important challenge in clinical work. The aim of the present study is to elucidate potential biomarkers and therapeutic targets for SCI-induced muscle atrophy (SIMA) using proteomic and bioinformatic analyses. The protein samples from rat soleus muscle were collected at different time points following SCI injury and separated by two-dimensional gel electrophoresis and compared with the sham group. The identities of these protein spots were analyzed by mass spectrometry (MS). MS demonstrated that 20 proteins associated with muscle atrophy were differentially expressed. Bioinformatic analyses indicated that SIMA changed the expression of proteins associated with cellular, developmental, immune system and metabolic processes, biological adhesion and localization. The results of the present study may be beneficial in understanding the molecular mechanisms of SIMA and elucidating potential biomarkers and targets for the treatment of muscle atrophy.

Introduction

Spinal cord injury (SCI) is a serious central nervous system disorder. Sociological changes, and infrastructural and transport system development have resulted in an increased incidence of SCI (1). Patients with SCI experience irreversible sensory and motor dysfunction. In modern society, the length of time that patients with paralysis and SCI survive has increased, which results in a heavy financial burden for the families and society.

Correspondence to: Professor Shi-Qing Feng, Department of Orthopaedics, Tianjin Medical University General Hospital, 154 Anshan Road, Heping, Tianjin 300052, P.R. China
E-mail: fengsq321@126.com

[*]Contributed equally

SCI commonly leads to muscle atrophy (2). Previous research has demonstrated that within the initial 6-18 months following SCI, 27 to 56% of the muscle fibers have atrophied (3). Currently, there is no clear consensus regarding classification of the type of atrophy that occurs following SCI, certain reports suggest disuse (4-7) and denervated atrophy (8,9). However, the atrophy induced by SCI is different from the aforementioned types of atrophy. Disuse models are based on variable degrees of unloading and inactivity, including ankle immobilization and hindlimb unloading. Disuse-induced muscle atrophy occurs when the central nervous system is intact. Another scenario is denervated atrophy, which is often induced by the model of peripheral axotomy (10,11). The central nervous system is not damaged in this type of muscle atrophy, as the injury is restricted to the axon of the dorsal root ganglion. The difference between SCI-induced muscle loss and the aforementioned types of atrophy is that in SCI the lower motor neurons remain intact and upper neurons cannot transmit information to the lower neurons.

Due to the complexity of the central nervous system and the observed cases of spontaneous functional recovery (12,13), the present study hypothesizes that the SCI-induced muscle atrophy (SIMA) may be the result of a special pathological mechanism. To develop novel treatment strategies or find novel diagnostic markers, it is required to investigate the molecular mechanisms and signaling pathways that mediate SCI-induced muscle atrophy. Previous studies have demonstrated the involvement of certain molecules and genes during this pathological process (14-16). However, the pathological mechanisms of SIMA are complex, thus, only investigating certain molecules is insufficient. Microarray data has provided some indication of the changes to mRNA expression levels that occur within the whole genome following SCI. However, the mRNA expression level does not always correlate with the protein expression level. Post-translational modifications and microRNAs may affect the protein expression levels (17). Thus, adopting a proteomics approach to analyze the global protein profile in SIMA may provide more accurate information that cannot be obtained from microarray analysis.

To the best of our knowledge, there have been no systematic studies aimed at identifying the proteins associated with SIMA on a proteome scale. The present study compared normal soleus muscle samples with post-SCI soleus muscle samples by two-dimensional (2D) gel electrophoresis,

followed by matrix assisted laser desorption/ionization-time of flight mass spectrometry (MALDI-TOF MS) analysis and identified a number of specific proteins that demonstrated differential expression levels. It is important to accumulate basic data, and the results of the present study may improve diagnostic procedures and the design of future strategies to treat SIMA.

Materials and methods

Animals and treatments. In the present study, female Wistar rats (n=30; weight, 220-250 g, age, 8 weeks; Tianjin Medical University, Tianjin, China) were used. Rats were single-housed in standard plastic cages in a room temperature (24±2°C), relative humidity (50±10%), and light/dark conditions (12/12-h light/dark cycle) room with access to food and water *ad libitum*. The study was approved by the ethics committee of Tianjin Medical University General Hospital. All procedures in the current study, including the use of experimental animals, followed the guidelines of the Animal Care and Research Committee of Tianjin Medical University. The rats were divided into a sham group and two injury groups (7 and 14 days post-SCI; n=10/group). The contusion injury models were induced by the standard New York University (NYU) impactor, as described previously (18). Animals were anesthetized (3 ml/kg 10% chloral hydrate, intraperitoneally) and laminectomized to expose the T10 spinal cord. A moderate injury was generated by dropping a metal rod (10 g, 12.5 mm) onto the back side of the spinal cord. The compression force and velocity were controlled by a surveillance system to maintain uniformity between animals. These rats were manually treated with bladder emptying. Sham subjects underwent a T10 laminectomy without contusion. Locomotive behavior was assessed at 0, 2, 4, 6, 8, 10, 12 and 14 days following injury using Basso, Beattie, and Bresnahan (BBB) score (19) to ensure that all subjects exhibited a normal curve of functional changes following SCI.

After 7 and 14 days, rats were euthanized with pentobarbital anesthesia (100 mg/kg, intraperitoneally), and then perfused with phosphate buffered-saline (PBS). Following perfusion, the posterior hind limbs were sliced to retrieve soleus muscle samples. Initially, the gastrocnemius muscle was lifted by cutting the terminus of the Achilles tendon to expose the soleus muscle. The soleus muscle was carefully excised from the posterior limbs and all connective tissue was removed to reserve muscles. Prior to each operation, the body weight of the rats was measured and then the isolated soleus muscle was weighed following bilateral harvesting. Following the surgery, the ratio of muscle weight to body weight was calculated, then muscle samples were frozen in liquid nitrogen and stored at -80°C. Control group rats were sacrificed following the same protocol at 14 days post-injury.

Histological examination. Samples from each group (n=10) were fixed in 10% phosphate-buffered formaldehyde solution. Following the process of decalcification and dehydration, the muscles were embedded in paraffin, cut into 5-μm sections and stained using hematoxylin and eosin. Muscle fibers (≥100 in each group) were observed in bright-field using Nikon ECLIPSE TS100 light microscope (Tokyo, Japan)

and Nikon D7200 image acquisition system. Their diameters were measured using Image J software (National Institutes of Health, Bethesda, MD, USA).

Sample preparation and 2D gel electrophoresis. Muscles samples were washed twice with PBS, once with distilled water and then ground to a fine powder with a pestle in liquid nitrogen. Lysis buffer [8 M urea, 2 M thiourea, 2% (w:v) CHAPS, 1% dithiothreitol (DTT), 1 mM phenylmethanesulfonyl fluoride (PMSF); 0.17 ml], 50 μg/ml DNase I and 1 mM PMSF was added to each sample. The samples were lysed by exposure to ultrasound for 30 sec (time interval 0.5 sec) repeated four times. The lysates were centrifuged at 12,000 x g for 30 min at 4°C to obtain the supernatants. Protein concentration was determined using the Bradford method and samples were stored at -80°C.

For first-dimension isoelectric focusing, pH 3-10 non-linear range immobilized pH gradient (IPG) strips (18 cm) were rehydrated with solubilized protein samples (800 μg) for 12 h. Isoelectric focusing was performed Isoelectric focusing was performed using the Protean II Xi cell electrophoresis system (Bio-Rad Laboratories, Inc., Hercules, CA, USA) under the following voltage time program: 0-500 V for 1 h, 500 V for 5 h, 500-3500 V for 3.5 h, 3500 V for 14 h and finally 3500-5000 V for 4 h.

Immediately following focusing, the IPG strips were equilibrated for 15 min in equilibration buffer I [50 mM Tris-HCl pH 6.8, 6 M urea, 30% glycerol, 2% sodium dodecyl sulfate (SDS), 2% DTT, 0.02% bromophenol blue], and then for 15 min in equilibration buffer II (50 mM Tris-HCl pH 6.8, 6 M urea, 30% glycerol, 2% SDS, 2.5% iodoacetamide, 0.02% bromophenol blue). The second dimension separation was performed at 15°C using a vertical electrophoresis system (Multiphor II; GE Healthcare Life Sciences , Chalfont, UK) with 1-mm 12.5% acrylamide gels run at 20 mA/gel until the tracking dye reached the bottom of the gel. The 2D PAGE gel was then stained with Coomassie Blue.

Visualization of proteins and image analysis. Following electrophoresis, the 2D gels were subjected to staining with a solution of 10% ammonium sulfate, 10% phosphoric acid, 0.12% G250 and 20% methanol overnight.

The gels were washed with a destaining solution (3% glacial acetic acid) in horizontal rotators. Finally, the gels were washed with Milli-Q water for 30 min. Images were obtained by scanning the 2D gels with a PowerLook 2100XL scanner (UMAX Technologies, Inc., Dallas, TX, USA).

PDQuest v 8.0 (Bio-Rad Laboratories, Inc.) software was used to calculate the intensities of protein spots to identify differentially expressed proteins. To correct quantitative variations in the intensity of protein spots, spot volumes were normalized as a percentage of the total volume of all the spots present in a gel. Only spots that were consistently present in the gels from at least three rats in each group were analyzed to avoid spot differences that were due to gel-to-gel or biological variation inherent among the rats. The protein molecular weight, which ranged from 10 to 100 kDa, and the isoelectric point (pI), which ranged from 3 to 10, of each protein spot were calculated by the software using the distributions of standard markers and pI positions, respectively.

Analysis of variance (AVOVA) with Tukey's post-hoc multiple comparison tests were performed to analyze statistically different intensities among groups. P<0.05 was considered to indicate a statistically significant difference.

In-gel tryptic digestion and MALDI-TOF-MS analysis. Selected protein spots were excised from the gel and cut into ~1 mm^2 pieces. Samples were destained using 50% (vv) acetonitrile (ACN) and 25 mM ammonium bicarbonate (100 μl, pH 8.0) for 15 min, this was repeated three times until the destaining process was complete. The gel samples were dipped into 100% ACN (30 μl, pH 8.0) for 5 min until they turned white. They were dried at room temperature and the samples were then digested using trypsin (8 μl, 0.005 mg/ml) at 37°C for 16 h. The digested proteins (0.3 μl) coupled with 0.3 μl matrix were subjected to MALDI-TOF MS analysis using a 4700 Proteomics Analyzer (Applied Biosystems; Thermo Fisher Scientific, Inc., Waltham, MA, USA) to obtain the peptide mass fingerprint (PMF) with 4,600 laser intensity. The peak list was generated by GPS Explorer v 3.5 software (Applied Biosystems; Thermo Fisher Scientific, Inc.) and searched using Mascot (version 2.1.0; Matrix Science Ltd., London, UK). The PMFs were processed by using the NCBI databases (www.ncbi.nlm.nih.gov) and the fingerprinting method was applied allowing a maximum of one missed tryptic cleavage per protein. The protein score confidence calculated using the Mascot algorithm. Confidence score ≥95% and P<0.05 was considered to indicate a statistically significant difference.

Classification of proteins. Identified proteins were submitted to the Protein Analysis Through Evolutionary Relationships (PANTHER) classification system (www.pantherdb.org) to determine their function via high-throughput analysis (20). Proteins were classified according to family and subfamily, molecular function, biological process and pathway.

Statistical analysis. Data are presented as the mean ± standard error of the mean. Significant differences were determined by ANOVA testing. SPSS software version 22.0 was used for data analysis (SPSS Inc., Chicago, IL, USA). P<0.05 was considered to indicate a statistically significant difference.

Results

BBB score in rats post-SCI increased with recovery time. In the control group, all rats exhibited a BBB score of 21. In the injured groups, immediately following SCI, the motor function of rats' hind limbs was severely impaired leading to BBB scores of ~0. Subsequently, the score gradually increased and all injured subjects demonstrated a similar recovery process. SCI rats recovered to exhibit BBB scores of ~9 by 7 days post-injury. Scores reached 10 after 14 days. Rats in the control group exhibited BBB scores of 21 throughout the experiment (Fig. 1).

SCI reduces soleus muscle fiber diameter. The mean diameter of the soleus muscle fiber was 94.4±10.8 μm in the control group. In the SCI groups, the mean diameters of the soleus muscle fiber were 76.7±10.0 μm and 66.2±8.2 μm at
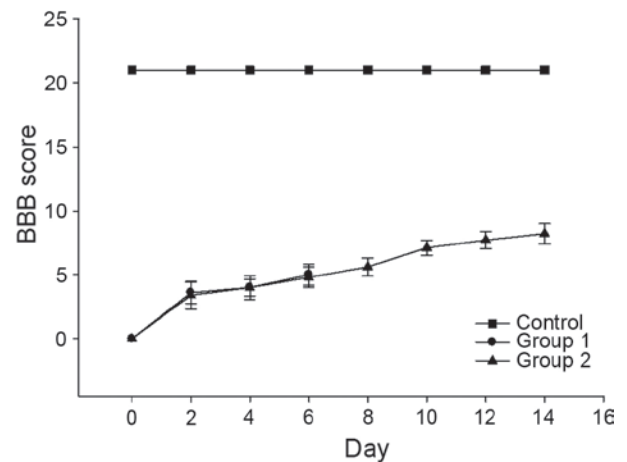

Figure 1. Locomotor behavior analysis by BBB score. Following spinal cord injury, the BBB score gradually increased. Data points present the mean ± standard error of the mean. BBB, Basso, Beattie, and Bresnahan.

7 and 14 days post-injury, respectively. The diameters in the SCI groups were significantly decreased compared with the control group (P<0.01). The mean diameter of the soleus muscle fiber decreased gradually at different time points (Fig. 2).

SCI induced differential protein expression in soleus muscle samples. Differentially expressed proteins in the soleus muscle of injured and control rats were identified and analyzed using 2D PAGE and MALDI TOF. Gel images of proteins isolated from the muscle of control, 7 and 14 days post-SCI groups were compared (Fig. 3). Per gel, >500 protein spots were detected. The protein expression profile in the soleus muscle of SCI rats indicated that the expression levels of >50 proteins were changed compared with the control group. Among altered proteins, 23 protein spots exhibited significant changes (Table I) and were quantitatively high enough to be identified by MALDI-TOF. MS data were analyzed using the Mascot search engine. The Mascot search identified 20 spots with high confidence (Table II). The confidence score of proteins was >95%.

To investigate the dynamic molecular mechanisms involved in SCI, the identified altered proteins were classified into 9 functional categories using the PANTHER database, including biological adhesion, cellular component organization or biogenesis, cellular processes, developmental processes, immune system processes, localization, metabolic processes, multicellular organism processes and response to stimulus (Fig. 4).

Discussion

Repeatable injuries are essential for assessing the severity of muscle atrophy in SCI animal models in original and replicative studies. The current study used an NYU impactor to generate the SCI and verified that SCI animals shared similar recovery curves, which were in accordance with the results of Basso *et al* (21). Furthermore, the BBB recovery curves were identical for the experimental groups at 14 days post-injury.
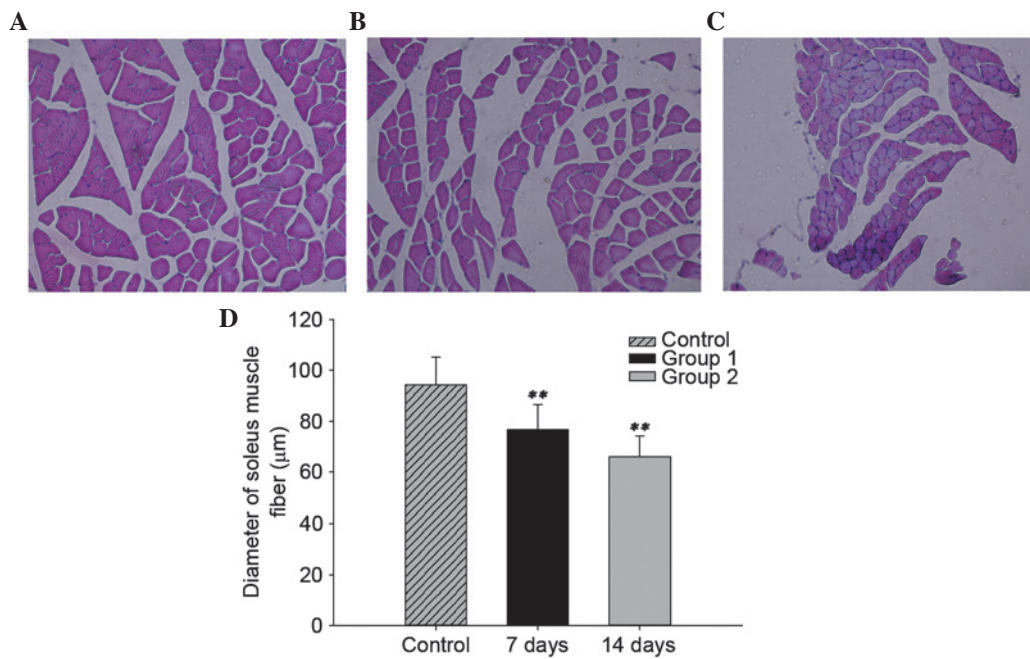
Figure 2. The mean diameter of the soleus muscle fiber at different time points following SCI. Hematoxylin and eosin staining (magnification x400) of (A) the control group, (B) group 1 (7 days post-SCI) and (C) group 2 (14 days post-SCI). (D) Quantitative analyses were performed to confirm the morphological results. Data are presented as the mean ± standard error of the mean. **$P<0.01$ vs. control group. SCI, spinal cord injury.
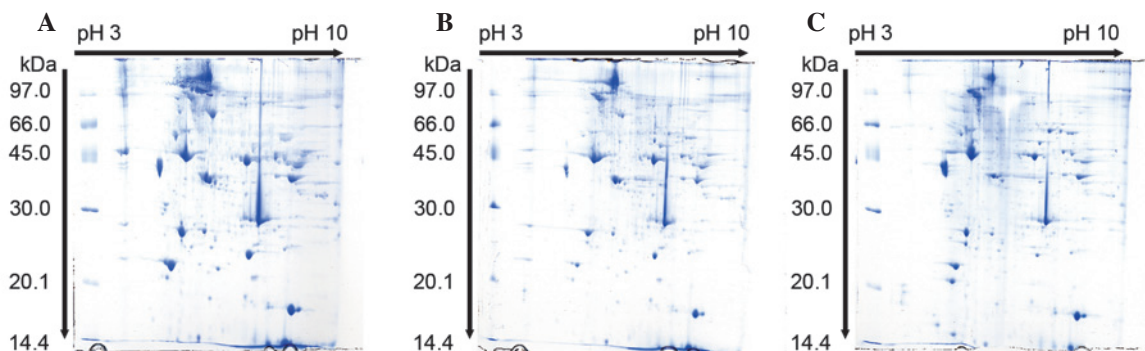

Figure 3. Protein profiles of 2D gel electrophoresis. 2D gels representing proteins from (A) the control group, (B) group 1 (7 days post-SCI) and (C) group 2 (14 days post-SCI). $P<0.05$, n=3. SCI, spinal cord injury.

This indicates that the present study produced a consistent and reproducible contusion SCI model.

Using 2D gels and MALDI-TOF MS analysis, the current study identified differentially expressed proteins in soleus muscle fibers of control and SCI model rats. In present study, it was demonstrated that this method is efficient for the identification of multiple proteins, a number of them at low abundance. Previous studies investigating muscle atrophy typically focus on the disuse and denervated animal models to simulate their corresponding clinical phenomenon. SIMA is often classified as one of these models of muscle atrophy or a combination of these models. However, the pathological process of SIMA involves multiple factors, including signal transduction, immunization, electrical conduction, stimuli and metabolism (22), which results in a complex condition that cannot be attributed to one molecular mechanisms or a simpler combination of a small number. Thus, the present study investigated the pathological changes that occur during

SIMA. Using 2D gels, numerous proteins were identified. Certain proteins exhibited a similar expression pattern as previously described (23), but others exhibited different curves or inconsistent ones (24). The potential importance and function of these proteins in SIMA is discussed further below.

The 14-3-3 proteins, as conserved regulatory molecules, have been demonstrated to be involved in numerous intracellular processes, including cell cycle regulation, metabolic control, apoptosis, and the control of gene transcription in almost all eukaryotic cells. Previous research demonstrated that 14-3-3 proteins are upregulated in the denervated tibialis anterior muscle of rats (25). However, other studies have observed that 14-3-3 was not increased in the skeletal muscles of patients with chronic obstructive pulmonary disease, which is a hypoxemic disease with similar characteristics to the early changes observed in the microenvironment during SCI (26). As a prognostic

Table I. Identification of differentially expressed proteins by MALDI-TOFMS in rat soleus muscle at different time points following SCI.

	Fold-change protein expression		
Protein name	7 days post-SCI/control	14 days post-SCI/control	14 days post-SCI/ 7 days post-SCI
Myosin regulatory light chain 2	0.157911	0.242524	0.651114
14-3-3 Protein ε	2.198649	1.282510	1.714334
Probable C>U-editing enzyme APOBEC-2	0.742312	2.545599	0.291606
Tropomyosin β chain	2.230306	0.752411	2.964213
ATP synthase β subunit	1.201723	3.443378	0.348995
Myosin light chain	0.247498	0.156377	1.582694
Myosin light chain 3	0.247498	0.156377	1.582694
α-Actinin-2	0.253011	0.070115	3.608539
Chain A, crystal structure of the 70-kDa heat shock cognate protein	0.455156	1.406490	0.323611
Heat shock protein β 6	0	1.292586	0
Serum albumin precursor	2.528853	2.490987	1.015201
α B-crystallin	+∞[a]	00[b]	0
Troponin T class IIIb β	+∞[a]	+∞[a]	0.326424
β-Enolase	+∞[a]	+∞[a]	0.117352
Creatine kinase M-type	+∞[a]	+∞[a]	2.717467
Fibrinogen β chain precursor	0.401764	0.946549	0.424452
Fibrinogen α chain	0.139896	1.026677	0.136261
MMSDH	0.127811	0.816477	0.156540
Phosphoglycerate kinase 1	0.081919	0.458707	0.178586

[a]The protein was only expressed post-SCI, thus the ratio between SCI and control is infinite. [b]The protein was not expressed at 14 days post-SCI or in the control. SCI, spinal cord injury; APOBEC-2, apolipoprotein B mRNA editing enzyme catalytic polypeptide like 2; MMSDH, aldehyde dehydrogenase 6 family member A1.

indicator, early accumulation of the 14-3-3 protein in the cerebrospinal fluid of patients with acute transverse myelitis was perceived to have been associated with little or no recovery of neurological function (27). However, deficiencies have been noted regarding certain aspects of these previous studies. The limited number of subjects (n=4 per group) may influence the accuracy of results. Furthermore, a previous study (28) observed that 14-3-3 protein was only expressed in ~10% of the patients and concluded that 14-3-3 expression was, thus, not associated with a poor patient outcome. Therefore, the present study hypothesizes that 14-3-3 may be important for the prediction of recovery from muscle atrophy following SCI. Certain studies support this hypothesis. In the cerebrospinal fluid of SCI rats, severe injury induced a slight reduction in 14-3-3 protein expression compared with moderate injury (29). Another study with a contusion model demonstrated that the expression levels of three isoforms of the 14-3-3 protein family increased at the mid-stage of the recovery following the restoration of bladder function (30). Despite the possibility that elevated levels of 14-3-3 protein following SCI may reflect the process of neuronal damage (31), in the central system (32) or peripheral tissues (33), the present results demonstrate that 14-3-3 protein, coupled with functional recovery, was increased despite an early decrease,
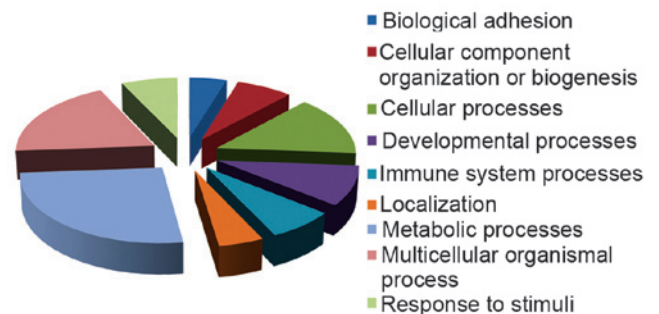

Figure 4. Functional classification of identified proteins in the soleus muscle of rats with SCI. Pie chart demonstrates functional classifications depending on the biological process related to each protein using Protein Analysis Through Evolutionary Relationships.

which may be attributed to the slow reaction of the protein. Upregulation of 14-3-3 protein expression levels can activate downstream reaction of the phosphatidylinositol-4,5-bisphosphate 3-kinase-AKT signaling pathway, which may suppress apoptosis. An aim of future research will be to investigate that underlying mechanism that results in changes to 14-3-3 expression levels following SCI. Different severities of SCI and more time points will be useful to elucidate

Table II. Identification of differentially expressed proteins by MALDI-TOF MS in rat soleus muscle samples at different time points following SCI.

SSP	Accession number	Protein name	MWpI[a]	Peptide count	Score[b]	Potential participation of signaling pathways
1108	386869343	Myosin regulatory light chain 2	18868.394.86	13	100	Focal adhesion, regulation of actin cytoskeleton
1306	13928824	14-3-3 Protein ε	29326.484.63	8	99.39	Hippo, PI3K-Akt, p53 signaling
1407	9507245	14-3-3 Protein ε	28455.984.8	11	100	Hippo, PI3K-Akt, p53 signaling
2102	157822795	Probable C>U-editing enzyme APOBEC-2	25871.964.75	12	100	Not annotated
2209	11875203	Tropomyosin β chain	32930.594.66	12	99.95	Cardiac muscle contraction, adrenergic signaling in cardiomyocytes
2617	1374715	ATP synthase β subunit	51170.654.92	22	100	Not annotated
3501	205474	Myosin light chain	20948.594.99	13	100	Focal adhesion, regulation of actin cytoskeleton
4108	6981240	Myosin light chain 3	22256.135.03	15	100	Focal adhesion, regulation of actin cytoskeleton
4406	157951643	α-Actinin-2	104338.545.31	41	100	Not annotated
5112	178847300	Chain A, crystal structure of the 70-kDa	59894.935.91	23	100	MAPK signaling pathway, heat shock cognate protein, endocytosis, protein processing in endoplasmic reticulum
5310	20302069	Heat shock protein β 6	17551.126.05	7	99.97	Nicotinate and nicotinamide metabolism
5406	158138568	Serum albumin precursor	70709.866.09	17	100	Metabolic pathways, endocrine and other factor-regulated calcium reabsorption, Ras and Rap1 signaling
5525	30387800	α B-crystallin	20155.446.84	16	100	Protein processing in endoplasmic reticulum
6517	207391	Troponin T class IIIb β	28301.929.36	15	100	Not annotated
6518	126723393	β-Enolase	47326.457.08	16	100	Not annotated
6520	6978661	Creatine kinase M-type	43219.876.58	31	100	Not annotated
7303	158186678	Fibrinogen β chain precursor	54827.927.9	24	100	Complement and coagulation cascades, platelet activation
1202	144922622	Fibrinogen α chain	60980.867.11	23	100	Endocytosis, complement and coagulation cascades, platelet activation
1205	400269	MMSDH	58226.748.47	12	100	Not annotated
1206	40254752	Phosphoglycerate kinase 1	44909.148.02	20	100	Glycolysisgluconeogenesis, HIF-1 signaling

[a]Values of MW and pI are from the database. [b]The sequence of matched peptide with the highest ion score and confidence interval %=100. MALDITOF MS, matrix-assisted laser desorptionionization time-of-flight mass spectrometry; SCI, spinal cord injury; SSP, significantly expressed spot number; MW, molecular weight; pI, isoelectric point; PI3K, phosphatidylinositol-4,5-bisphosphate 3-kinase; Akt, v-akt murine thymoma viral oncogene; APOBEC-2, apolipoprotein B mRNA editing enzyme catalytic polypeptide like 2; MAPK, mitogen-activated protein kinase; Ras, rat sarcoma viral oncogene homolog; Rap1, RAP1A, member of RAS oncogene family; MMSDH, aldehyde dehydrogenase 6 family member A1; HIF-1, hypoxia inducible factor 1.

the biochemical and pathophysiological function of proteins differentially expressed in SIMA.

αB-crystallin (CryAB) is a small heat shock protein involved in preventing protein aggregation (34). Dysfunction of CryAB may result in skeletal muscle disorders and enhancing the function of this protein is accepted as a potential therapeutic strategy (35). Previous studies indicate that CryAB is a protective protein that maintains the capability of satellite cells to regenerate skeletal muscle (34) and that it is important for muscle homeostasis (36). Denervated tibialis anterior muscle exhibits increased expression of CryAB. CryAB can prevent apoptosis induced by a variety of stimuli, which may explain why fast-twitch anterior muscle exhibits reduced atrophy (25). In the present study, CryAB protein expression was upregulated at 7 days post-SCI and then reduced to the level as that of the control by day 14. This notable finding is contrary to previous research that demonstrated that denervation decreased the expression levels of CryAB in slow muscle, particularly in the soleus (37). However, this discrepancy suggests that SIMA, which differs from denervation, has the potential for recovery at an early stage and that the upregulation of CryAB may be a marker of protection. This hypothesis is supported by indirect evidence demonstrating that expression of CryAB returned to the level observed in the normal controls following successful reinnervation (38). Together, the results of the present study indicate that, following SCI, there is a transient time window for the self-restoration of skeletal muscle, but ultimately the positive effect is suppressed by persistent disadvantageous pathogenic factors. Thus, confirming the accurate time window and the upregulation of CryAB may be investigated as future therapeutic strategies.

β-enolase is widely distributed in cells and involved in the glycolysis pathway (39). Increasing evidence has demonstrated that β-enolase may assist DNA transcription, replication and repair. Previous studies demonstrated that the expression of β-enolase is dependent on regular nerve activity (40) and its upregulation indicates regeneration of skeletal muscle (41). Research indicates that the expression of β-enolase following denervation remains at a low level in slow-twitch muscle, however, continues to decrease in the fast-twitch muscle (40,42). However, the present study demonstrated that the expression levels of β-enolase in SCI muscle increased steadily, which indicates that SIMA has the reverse effect on this protein. Previous evidence suggested that following reinnervation, the expression level of β-enolase in soleus muscle increased, which may support the hypothesis that the increase of β-enolase expression in the soleus muscle depends on the integrity of peripheral nerves. However, the functional recovery of SCI is limited and muscle atrophy is inevitable. In sum, the present study hypothesized that the role of β-enolase is altering the muscle types, as demonstrated in a previous study (43) that supports the current observations. In addition, a longer period of observation is required in future research.

The bio-functions of apolipoprotein B mRNA editing enzyme catalytic polypeptide like 2 (APOBEC2) have been hypothesized to include mediation of the cytidine-to-uridine transcriptional editing of mRNA (44). Due to exclusive expression in skeletal and cardiac muscles, APOBEC2 was suggested to be important in the physiological function of intramuscular development. However, APOBEC2 knockout mice did not exhibit a change in phenotype (45). This may indicate that APOBEC2 subtly regulates certain aspects of muscle function, including the response to damage stimuli. The results of the present study demonstrated that the protein expression levels of APOBEC2 in the soleus increased gradually following SCI, in contrast to the change in expression levels during denervation atrophy (24). This finding may be attributed to intact neurons that give priority to compensation of muscle function by switching the muscle types. A previous study demonstrated that APOBEC2-deficient mice exhibited a marked shift in muscle fiber type, from fast to slow (46). It is hypothesized that the increase of APOBEC2 expression levels may result in enhanced conversion of slow fibers to fast ones. Further evidence indicates that the ratio of slow to fast fibers in soleus muscle was decreased gradually following spinal cord transection (47).

α-actinin-2 is a major Z-disk component, which is crucial for the crosslinking of actin and titin filaments (48,49). It is understood that α-actinin-2 is expressed in all types of muscle fibers, including slow and fast fibers (50). Previous studies demonstrated that α-actinin-2 can bond with calsarcin-2, a key inhibitor of calcineurin activation, to release calcineurin from calsarcin-2 and change the fast fibers to a slow phenotype (51-53). The present study demonstrated that following SCI, the expression of α-actinin-2 in the soleus dropped sharply over time. This decrease indicates that downregulation of α-actinin-2 may result in enhancement of calsarcin-2, which inhibits the activation of calcineurin signaling, and a shift in fiber type from slow to fast. The results of the current study are consistent with previous research and it is hypothesized that the shift of metabolic phenotype of muscle fibers following SCI preserves the energy metabolism and function of the muscle.

Heat shock protein family A member 4 (Hsp70) is a highly conserved molecular chaperone protein that has been reported to regulate various processes associated with stress, damage or degeneration (54). The protective effects of Hsp70 in muscle atrophy have also been demonstrated in a number of previous studies (55-57). Upregulation of Hsp70 may prevent muscle atrophy as a result of denervation, aging or disuse (58-60). The present study observed that the expression of Hsp70 in the soleus muscle was slightly reduced at 7 days post-SCI and then increased sharply at 14 days to a level markedly higher than that of the control. This indicates that the muscle exhibited the potential for restoration following central nervous system injury. The slight reduction observed at the early stage of SCI may be attributed to a temporary disorder of energy metabolism (61) or inhibition of glucocorticoid due to the stress response (62). However, it remains necessary to investigate why the protective effect of Hsp70 is too limited to prevent atrophy and whether the increased expression of this protein is also a transient phenomenon.

Another notable finding from the present study is that the protein levels of certain myosin regulatory light chain (MLC) isoforms and enzymes involved in cellular and metabolic processes were decreased in the soleus muscle at early stages (7 days) post-SCI. Subsequently, the expression was increased at 14 days post-SCI, with certain isoforms almost at similar

levels to the control. The function of MLCs is associated with contractile force and velocity in muscle fibers (63). Multiple reports have demonstrated that the changes to MLCs were associated with fiber-type shift (8,64-66). Certain enzymes key in cellular and metabolic processes, including fibrinogen α and β chain, aldehyde dehydrogenase 6 family member A1 and phosphoglycerate kinase 1, participate in various biological processes and their normal function is for homeostasis of physiological and pathological metabolism (67-69). Fluctuations in the expression levels of these proteins may indicate that skeletal muscle has been damaged by central nervous system injury, but with relatively integrated peripheral nervous control, will exhibit reduced function of multiple molecular processes at an early stage and subsequently adapt during the middle stage. The results of the current study are in accordance with a previous study that demonstrated that muscle appears to have plasticity and can adapt following moderate spinal cord contusion, which was similar to the present animal model (70).

The data of the current study indicated that SCI-induced atrophic muscles exhibited limited molecular improvements, which may be associated with functional recovery. However these improvements cannot reverse the changes to the size of muscle fibers of the soleus muscles of SCI rats. It is accepted that following moderate contusion, rats will exhibit spontaneous recovery of motor function following a fixed pattern (71,72). Furthermore, previous findings indicated that the growth effects of muscle fibers may result in improvement of motor function (73-75), however, this does not mean that the size of the fibers is directly associated with BBB score. Notably, the results of the present study demonstrated that the extent of variation in the second week was reduced compared with the change in the first week, which may be attributed to the temporary molecular compensatory mechanisms. These mechanisms may be used as therapeutic targets to induce anti-atrophic effects or reverse the effects on skeletal muscle, potentially coupled with more observable improvement of motor function (34,62). However, in the current study, due to specific molecular improvements, the process of muscle atrophy slowed at a later stage, however, it may not be able to be stopped or reversed. In addition, the increases to BBB scores also slowed down at this stage. Concerning the delayed effects of molecules prior to phenotypic changes, it is concluded that the decreased extent of atrophic response was consistent with the sharp increase to motor function recovery at the early stage. Future studies are required to investigate prolonged observation over increased time points.

In conclusion, the current study used a proteomics approach to identify differential expression of proteins in the soleus muscle at different time points following SCI. The identified proteins were associated with biological adhesion, cellular processes, developmental processes, immune system processes, localization and metabolic processes. The results of the present study demonstrated that SIMA has characteristics different to disuse and denervated atrophy, or a combination of them. The present study may improve the understanding of the association between central nervous system injury and skeletal muscle atrophy. Furthermore, the results may provide insight into potential mechanisms or cellular pathways that may be adopted as biomarkers and targets for the treatment of SIMA.

References

1. van den Berg ME, Castellote JM, Mahillo-Fernandez I and de Pedro-Cuesta J: Incidence of spinal cord injury worldwide: A systematic review. Neuroepidemiology 34: 184-192, 2010.
2. Taillandier D, Aurousseau E, Meynial-Denis D, Bechet D, Ferrara M, Cottin P, Ducastaing A, Bigard X, Guezennec CY, Schmid HP and Attaix D: Coordinate activation of lysosomal, Ca²⁺-activated and ATP-ubiquitin-dependent proteinases in the unweighted rat soleus muscle. Biochem J 316: 65-72, 1996.
3. Castro MJ, Apple DF Jr, Rogers S, Dudley GA. Influence of complete spinal cord injury on skeletal muscle mechanics within the first 6 months of injury. Eur J Appl Physiol 81:128-131, 2000.
4. Bodine SC: Disuse-induced muscle wasting. Int J Biochem Cell Biol 45: 2200-2208, 2013.
5. Booth FW and Gollnick PD: Effects of disuse on the structure and function of skeletal muscle. Med Sci Sports Exerc 15: 415-420, 1983.
6. Ohira Y, Yoshinaga T, Nomura T, Kawano F, Ishihara A, Nonaka I, Roy RR and Edgerton VR: Gravitational unloading effects on muscle fiber size, phenotype and myonuclear number. Adv Space Res 30: 777-781, 2002.
7. Roy RR, Baldwin KM and Edgerton VR: The plasticity of skeletal muscle: Effects of neuromuscular activity. Exerc Sport Sci Rev 19: 269-312, 1991.
8. Furuno K, Goodman MN and Goldberg AL: Role of different proteolytic systems in the degradation of muscle proteins during denervation atrophy. J Biol Chem 265: 8550-8557, 1990.
9. Midrio M, Danieli-Betto D, Megighian A, Velussi C, Catani C and Carraro U: Slow-to-fast transformation of denervated soleus muscle of the rat, in the presence of an antifibrillatory drug. Pflugers Arch 420: 446-450, 1992.
10. Goldberg AL: Protein turnover in skeletal muscle. II. Effects of denervation and cortisone on protein catabolism in skeletal muscle. J Biol Chem 244: 3223-3229, 1969.
11. Goldspink DF: The effects of denervation on protein turnover of rat skeletal muscle. Biochem J 156: 71-80, 1976.
12. Gonzalez-Rothi EJ, Rombola AM, Rousseau CA, Mercier LM, Fitzpatrick GM, Reier PJ, Fuller DD and Lane MA: Spinal interneurons and forelimb plasticity after incomplete cervical spinal cord injury in adult rats. J Neurotrauma 32: 893-907, 2015.
13. Kaegi S, Schwab ME, Dietz V and Fouad K: Electromyographic activity associated with spontaneous functional recovery after spinal cord injury in rats. Eur J Neurosci 16: 249-258, 2002.
14. Kostovski E, Boon H, Hjeltnes N, Lundell LS, Ahlsén M, Chibalin AV, Krook A, Iversen PO and Widegren U: Altered content of AMP-activated protein kinase isoforms in skeletal muscle from spinal cord injured subjects. Am J Physiol Endocrinol Metab 305: E1071-E1080, 2013.
15. Park S, Hong Y, Lee Y, Won J, Chang KT and Hong Y: Differential expression of caveolins and myosin heavy chains in response to forced exercise in rats. Lab Anim Res 28: 1-9, 2012.
16. Qin W, Bauman WA and Cardozo C: Bone and muscle loss after spinal cord injury: Organ interactions. Ann NY Acad Sci 1211: 66-84, 2010.
17. Wu Y, Collier L, Qin W, Creasey G, Bauman WA, Jarvis J and Cardozo C: Electrical stimulation modulates Wnt signaling and regulates genes for the motor endplate and calcium binding in muscle of rats with spinal cord transection. BMC Neurosci 14: 81, 2013.
18. Hill CE, Beattie MS and Bresnahan JC: Degeneration and sprouting of identified descending supraspinal axons after contusive spinal cord injury in the rat. Exp Neurol 171: 153-169, 2001.

19. Basso DM, Beattie MS and Bresnahan JC: A sensitive and reliable locomotor rating scale for open field testing in rats. J Neurotrauma 12: 1-21, 1995.
20. Mi H, Lazareva-Ulitsky B, Loo R, Kejariwal A, Vandergriff J, Rabkin S, Guo N, Muruganujan A, Doremieux O, Campbell MJ, Kitano H and Thomas PD: The PANTHER database of protein families, subfamilies, functions and pathways. Nucleic Acids Res 33:D284-D288, 2005.
21. Basso DM, Beattie MS, Bresnahan JC, Anderson DK, Faden AI, Gruner JA, Holford TR, Hsu CY, Noble LJ, Nockels R, et al: MASCIS evaluation of open field locomotor scores: Effects of experience and teamwork on reliability. Multicenter Animal Spinal Cord Injury Study. J Neurotrauma 13: 343-359, 1996.
22. Bickel CS, Slade JM, Haddad F, Adams GR and Dudley GA: Acute molecular responses of skeletal muscle to resistance exercise in able-bodied and spinal cord-injured subjects. J Appl Physiol (1985) 94: 2255-2262, 2003.
23. Johnston TE, Modlesky CM, Betz RR and Lauer RT: Muscle changes following cycling and/or electrical stimulation in pediatric spinal cord injury. Arch Phys Med Rehabil 92: 1937-1943, 2011.
24. Sato Y, Shimizu M, Mizunoya W, Wariishi H, Tatsumi R, Buchman VL and Ikeuchi Y: Differential expression of sarcoplasmic and myofibrillar proteins of rat soleus muscle during denervation atrophy. Biosci Biotechnol Biochem 73: 1748-1756, 2009.
25. Sun H, Li M, Gong L, Liu M, Ding F and Gu X: iTRAQ-coupled 2D LC-MSMS analysis on differentially expressed proteins in denervated tibialis anterior muscle of Rattus norvegicus. Mol Cell Biochem 364: 193-207, 2012.
26. Favier FB, Costes F, Defour A, Bonnefoy R, Lefai E, Baugé S, Peinnequin A, Benoit H and Freyssenet D: Downregulation of Akt/mammalian target of rapamycin pathway in skeletal muscle is associated with increased REDD1 expression in response to chronic hypoxia. Am J Physiol Regul Integr Comp Physiol 298: R1659-R1666, 2010.
27. Irani DN and Kerr DA: 14-3-3 protein in the cerebrospinal fluid of patients with acute transverse myelitis. Lancet 355: 901, 2000.
28. de Seze J, Peoc'h K, Ferriby D, Stojkovic T, Laplanche JL and Vermersch P: 14-3-3 Protein in the cerebrospinal fluid of patients with acute transverse myelitis and multiple sclerosis. J Neurol 249: 626-627, 2002.
29. Lubieniecka JM, Streijger F, Lee JH, Stoynov N, Liu J, Mottus R, Pfeifer T, Kwon BK, Coorssen JR, Foster LJ, et al: Biomarkers for severity of spinal cord injury in the cerebrospinal fluid of rats. PLoS One 6: e19247, 2011.
30. Lee JY, Kim BJ, Sim G, Kim GT, Kang D, Jung JH, Hwa JS, Kwak YJ, Choi YJ, Park YS, et al: Spinal cord injury markedly altered protein expression patterns in the affected rat urinary bladder during healing stages. J Korean Med Sci 26: 814-823, 2011.
31. Cuadrado-Corrales N, Jiménez-Huete A, Albo C, Hortigüela R, Vega L, Cerrato L, Sierra-Moros M, Rábano A, de Pedro-Cuesta J and Calero M: Impact of the clinical context on the 14-3-3 test for the diagnosis of sporadic CJD. BMC Neurol 6: 25, 2006.
32. Namikawa K, Su Q, Kiryu-Seo S and Kiyama H: Enhanced expression of 14-3-3 family members in injured motoneurons. Res Mol Brain Res 55: 315-320, 1998.
33. Peoc'h K, Beaudry P, Lauprêtre N and Laplanche JL: CSF detection of the 14-3-3 protein in unselected patients with dementia. Neurology 58: 509-510, 2002.
34. Neppl RL, Kataoka M and Wang DZ: Crystallin-αB regulates skeletal muscle homeostasis via modulation of argonaute2 activity. J Biol Chem 289: 17240-17248, 2014.
35. Sanbe A: Molecular mechanisms of α-crystallinopathy and its therapeutic strategy. Biol Pharm Bull 34: 1653-1658, 2011.
36. Singh BN, Rao KS and Rao ChM: Ubiquitin-proteasome-mediated degradation and synthesis of MyoD is modulated by alphaB-crystallin, a small heat shock protein, during muscle differentiation. Biochim Biophys Acta 1803: 288-299, 2010.
37. Atomi Y, Yamada S and Nishida T: Early changes of alpha B-crystallin mRNA in rat skeletal muscle to mechanical tension and denervation. Biochem Biophys Res Commun 181: 1323-1330, 1991.
38. Tews DS, Goebel HH, Schneider I, Gunkel A, Stennert E and Neiss WF: Expression profile of stress proteins, intermediate filaments, and adhesion molecules in experimentally denervated and reinnervated rat facial muscle. Exp Neurol 146: 125-134, 1997.
39. Gomes RA, Vicente Miranda H, Silva MS, Graça G, Coelho AV, Ferreira AE, Cordeiro C and Freire AP: Yeast protein glycation in vivo by methylglyoxal. Molecular modification of glycolytic enzymes and heat shock proteins. FEBS J 273: 5273-5287, 2006.
40. Nozais M, Merkulova T, Keller A, Janmot C, Lompré AM, D'Albis A and Lucas M: Denervation of rabbit gastrocnemius and soleus muscles: Effect on muscle-specific enolase. Eur J Biochem 263: 195-201, 1999.
41. Merkulova T, Dehaupas M, Nevers MC, Creminon C, Alameddine H and Keller A: Differential modulation of alpha, beta and gamma enolase isoforms in regenerating mouse skeletal muscle. Eur J Biochem 267: 3735-3743, 2000.
42. Kato K, Shimizu A, Semba R and Satoh T: Tissue distribution, developmental profiles and effect of denervation of enolase isozymes in rat muscles. Biochim Biophys Acta 841: 50-58, 1985.
43. Matsushita H, Yamada S, Satoh T, Kato K and Adachi M: Muscle-specific beta-enolase concentrations after cross- and random innervation of soleus and extensor digitorum longus in rats. Exp Neurol 93: 84-91, 1986.
44. Liao W, Hong SH, Chan BH, Rudolph FB, Clark SC and Chan L: APOBEC-2, a cardiac- and skeletal muscle-specific member of the cytidine deaminase supergene family. Biochem Biophys Res Commun 260: 398-404, 1999.
45. Mikl MC, Watt IN, Lu M, Reik W, Davies SL, Neuberger MS and Rada C: Mice deficient in APOBEC2 and APOBEC3. Mol Cell Biol 25: 7270-7277, 2005.
46. Sato Y, Probst HC, Tatsumi R, Ikeuchi Y, Neuberger MS and Rada C: Deficiency in APOBEC2 leads to a shift in muscle fiber type, diminished body mass, and myopathy. J Biol Chem 285: 7111-7118, 2010.
47. Dupont-Versteegden EE, Houlé JD, Gurley CM and Peterson CA: Early changes in muscle fiber size and gene expression in response to spinal cord transection and exercise. Am J Physiol 275: C1124-C1133, 1998.
48. Ribeiro EA Jr, Pinotsis N, Ghisleni A, Salmazo A, Konarev PV, Kostan J, Sjöblom B, Schreiner C, Polyansky AA, Gkougkoulia EA, et al: The structure and regulation of human muscle α-actinin. Cell 159: 1447-1460, 2014.
49. Takada F, Vander Woude DL, Tong HQ, Thompson TG, Watkins SC, Kunkel LM and Beggs AH: Myozenin: An alpha-actinin- and gamma-filamin-binding protein of skeletal muscle Z lines. Proc Natl Acad Sci USA 98: 1595-1600, 2001.
50. Ichinoseki-Sekine N, Yoshihara T, Kakigi R, Ogura Y, Sugiura T and Naito H: Fiber-type specific expression of α-actinin isoforms in rat skeletal muscle. Biochem Biophys Res Commun 419: 401-404, 2012.
51. Chin ER, Olson EN, Richardson JA, Yang Q, Humphries C, Shelton JM, Wu H, Zhu W, Bassel-Duby R and Williams RS: A calcineurin-dependent transcriptional pathway controls skeletal muscle fiber type. Genes Dev 12: 2499-2509, 1998.
52. Frey N, Richardson JA and Olson EN: Calsarcins, a novel family of sarcomeric calcineurin-binding proteins. Proc Natl Acad Sci USA 97: 14632-14637, 2000.
53. Seto JT, Quinlan KG, Lek M, Zheng XF, Garton F, MacArthur DG, Hogarth MW, Houweling PJ, Gregorevic P, Turner N, et al: ACTN3 genotype influences muscle performance through the regulation of calcineurin signaling. J Clin Invest 123: 4255-4263, 2013.
54. Liu Y, Gampert L, Nething K and Steinacker JM: Response and function of skeletal muscle heat shock protein 70. Front Biosci 11: 2802-2827, 2006.
55. Krawiec BJ, Frost RA, Vary TC, Jefferson LS and Lang CH: Hindlimb casting decreases muscle mass in part by proteasome-dependent proteolysis but independent of protein synthesis. Am J Physiol Endocrinol Metab 289: E969-E980, 2005.
56. Milne KJ and Noble EG: Exercise-induced elevation of HSP70 is intensity dependent. J Appl Phsiol (1985) 93: 561-568, 2002.
57. Thompson HS, Scordilis SP, Clarkson PM and Lohrer WA: A single bout of eccentric exercise increases HSP27 and HSCHSP70 in human skeletal muscle. Physiol Scand 171: 187-193, 2001.
58. Evertsson K, Fjällström AK, Norrby M and Tågerud S: p38 mitogen-activated protein kinase and mitogen-activated protein kinase-activated protein kinase 2 (MK2) signaling in atrophic and hypertrophic denervated mouse skeletal muscle. J Mol Signal 9: 2, 2014.
59. Senf SM, Dodd SL and Judge AR: FOXO signaling is required for disuse muscle atrophy and is directly regulated by Hsp70. Am J Physiol Cell Physiol 298: C38-C45, 2010.
60. Senf SM, Dodd SL, McClung JM and Judge AR: Hsp70 overexpression inhibits NF-kappaB and Foxo3a transcriptional activities and prevents skeletal muscle atrophy. FASEB J 22: 3836-3845, 2008.

61. Macario AJ and Conway de Macario E: Molecular chaperones: Multiple functions, pathologies, and potential applications. Front Biosci 12: 2588-2600, 2007.
62. Kukreti H, Amuthavalli K, Harikumar A, Sathiyamoorthy S, Feng PZ, Anantharaj R, Tan SL, Lokireddy S, Bonala S, Sriram S, *et al*: Muscle-specific microRNA1 (miR1) targets heat shock protein 70 (HSP70) during dexamethasone-mediated atrophy. J Biol Chem 288: 6663-6678, 2013.
63. Stevens L, Firinga C, Gohlsch B, Bastide B, Mounier Y and Pette D: Effects of unweighting and clenbuterol on myosin light and heavy chains in fast and slow muscles of rat. Am J Physiol Cell Physiol 279: C1558-C1563, 2000.
64. Gosker HR, Zeegers MP, Wouters EF and Schols AM: Muscle fibre type shifting in the vastus lateralis of patients with COPD is associated with disease severity: A systematic review and meta-analysis. Thorax 62: 944-949, 2007.
65. Nwoye L, Mommaerts WF, Simpson DR, Seraydarian K and Marusich M: Evidence for a direct action of thyroid hormone in specifying muscle properties. Am J Physiol 242: R401-R408, 1982.
66. Bozzo C, Stevens L, Toniolo L, Mounier Y and Reggiani C: Increased phosphorylation of myosin light chain associated with slow-to-fast transition in rat soleus. Am J Physiol Cell Physiol 285: C575-C583, 2003.
67. Huang YH, Tsai MM and Lin KH: Thyroid hormone dependent regulation of target genes and their physiological significance. Chang Gung Med J 31: 325-334, 2008.
68. Stines-Chaumeil C, Talfournier F and Branlant G: Mechanistic characterization of the MSDH (methylmalonate semialdehyde dehydrogenase) from *Bacillus subtilis*. Biochem J 395: 107-115, 2006.
69. Ahmad SS, Glatzle J, Bajaeifer K, Bühler S, Lehmann T, Königsrainer I, Vollmer JP, Sipos B, Ahmad SS, Northoff H, *et al*: Phosphoglycerate kinase 1 as a promoter of metastasis in colon cancer. Int J Oncol 43: 586-590, 2013.
70. Hutchinson KJ, Linderman JK and Basso DM: Skeletal muscle adaptations following spinal cord contusion injury in rat and the relationship to locomotor function: A time course study. J Neurotrauma 18: 1075-1089, 2001.
71. Hill CE, Brodak DM and Bartlett Bunge M: Dissociated predegenerated peripheral nerve transplants for spinal cord injury repair: A comprehensive assessment of their effects on regeneration and functional recovery compared to Schwann cell transplants. J Neurotrauma 29: 2226-2243, 2012.
72. Fouad K, Hurd C and Magnuson DS: Functional testing in animal models of spinal cord injury: Not as straight forward as one would think. Front Integr Neurosci 7: 85, 2013.
73. Jayaraman A, Liu M, Ye F, Walter GA and Vandenborne K: Regenerative responses in slow- and fast-twitch muscles following moderate contusion spinal cord injury and locomotor training. Eur J Appl Phsiol 113: 191-200, 2013.
74. Park S, Lee SK, Park K, Lee Y, Hong Y, Lee S, Jeon JC, Kim JH, Lee SR, Chang KT and Hong Y: Beneficial effects of endogenous and exogenous melatonin on neural recon-struction and functional recovery in an animal model of spinal cord injury. J Pineal Res 52: 107-119, 2012.
75. Stevens JE, Liu M, Bose P, O'Steen WA, Thompson FJ, Anderson DK and Vandenborne K: Changes in soleus muscle function and fiber morphology with one week of locomotor training in spinal cord contusion injured rats. J Neurotrauma 23: 1671-1681, 2006.